JOURNAL OF THE ROYAL SOCIETY Interface

Physical basis for the adaptive flexibility of *Bacillus* spore coats

Ozgur Sahin, Ee Hou Yong, Adam Driks and L. Mahadevan

J. R. Soc. Interface 2012 **9**, doi: 10.1098/rsif.2012.0470 first published online 1 August 2012

JOURNAL OF THE ROYAL SOCIETY Interface

J. R. Soc. Interface (2012) **9**, 3156–3160
doi:10.1098/rsif.2012.0470
Published online 1 August 2012

REPORT

Physical basis for the adaptive flexibility of *Bacillus* spore coats

Ozgur Sahin[1,*], Ee Hou Yong[2], Adam Driks[4] and L. Mahadevan[1,2,3]

[1]*Wyss Institute for Biologically Inspired Engineering, Harvard University, Boston, MA 02115, USA*
[2]*Department of Physics, School of Engineering and Applied Sciences, and* [3]*Department of Organismic and Evolutionary Biology, Harvard University, Cambridge, MA 02138, USA*
[4]*Department of Microbiology and Immunology, Loyola University Medical Center, 2160 S. First Avenue, Maywood, IL 60153, USA*

Bacillus spores are highly resistant dormant cells formed in response to starvation. The spore is surrounded by a structurally complex protein shell, the coat, which protects the genetic material. In spite of its dormancy, once nutrient is available (or an appropriate physical stimulus is provided) the spore is able to resume metabolic activity and return to vegetative growth, a process requiring the coat to be shed. Spores dynamically expand and contract in response to humidity, demanding that the coat be flexible. Despite the coat's critical biological functions, essentially nothing is known about the design principles that allow the coat to be tough but also flexible and, when metabolic activity resumes, to be efficiently shed. Here, we investigated the hypothesis that these apparently incompatible characteristics derive from an adaptive mechanical response of the coat. We generated a mechanical model predicting the emergence and dynamics of the folding patterns uniformly seen in *Bacillus* spore coats. According to this model, spores carefully harness mechanical instabilities to fold into a wrinkled pattern during sporulation. Owing to the inherent nonlinearity in their formation, these wrinkles persist during dormancy and allow the spore to accommodate changes in volume without compromising structural and biochemical integrity. This characteristic of the spore and its coat may inspire design of adaptive materials.

Keywords: bacterial spores; coat; folding; mechanical instability; wrinkles

*Author for correspondence (sahin@columbia.edu).

Electronic supplementary material is available at http://dx.doi.org/10.1098/rsif.2012.0470 or via http://rsif.royalsocietypublishing.org.

1. INTRODUCTION

Bacillus spores are dormant cells that exhibit high resistance to environmental stresses [1]. Spores consist of multiple concentric shells encasing dehydrated genetic material at the centre (the core). One of these shells is a loosely cross-linked peptidoglycan layer, called the cortex, surrounding the core. Encasing this is the coat, which exhibits a unique folding geometry (figure 1*a–c*). The coat protects the genetic material while permitting the diffusion of water and small molecules to the spore interior. Paradoxically, the coat must be chemically resilient and physically tough [5–7] but still possess significant mechanical flexibility [4,8,9]. During germination, the coat must be broken apart so that it can be rapidly shed [10].

The ridges of the *Bacillus subtilis* coat emerge during the process of sporulation in which water is expelled from the spore core and cross links occur in the cortex [5,10–14]. The mature spore is not static. It expands and contracts in response to changes in relative humidity [4,8,9]. Although ridges are present in spores of many if not most species [2,15–17] of the family *Bacillaceae*, these ridges are very poorly understood; we do not understand the forces guiding their formation, how their topography is influenced by the coat's material properties or their biological function, if any.

To address these questions, we first considered that ridges could emerge spontaneously, as in the case of wrinkles that form when a thin layer of material that adheres weakly to a support is under compression [18]. The coat and cortex form such a system, because the core volume (and, therefore, its surface area) decreases during sporulation [19]. Rucks can form if the stress in the system overcomes the adhesive forces between the coat and the underlying cortex [20]. Consequently, we investigated the role of mechanical instabilities in the formation of ridges and the implications of this mechanism for spore persistence.

2. RESULTS

The height profiles of a *B. subtilis* in figure 1*d* show that a partial unfolding of the ridges accompanies the expansion of the spore at high humidity. We obtained similar results for *Bacillus anthracis* spores (figure 1*e*). Furthermore, fully hydrated *Bacillus atrophaeus* spores were previously shown to exhibit similar characteristics [4], indicating that this behaviour is not limited to a single species and raising the possibility that it is ubiquitous.

To analyse whether ruck formation can explain the characteristic wrinkle patterns and their response to increased relative humidity, we modelled the coat and cortex as two adhered concentric rings and calculated the response of this structure to gradual reductions in volume, using a combination of scaling analyses and numerical simulations (see the electronic supplementary material). We restricted our model to two dimensions, both because the wrinkle morphology is that of long ridges along the spore, and in order to focus on a minimal model. Typical parameter values in our model are as follows: spore radius R_{coat}, and thickness, h, of the coat to be approximately 300 and 40 nm, respectively [2,21,22] (see the electronic supplementary material, table S1),

Received 12 June 2012
Accepted 11 July 2012

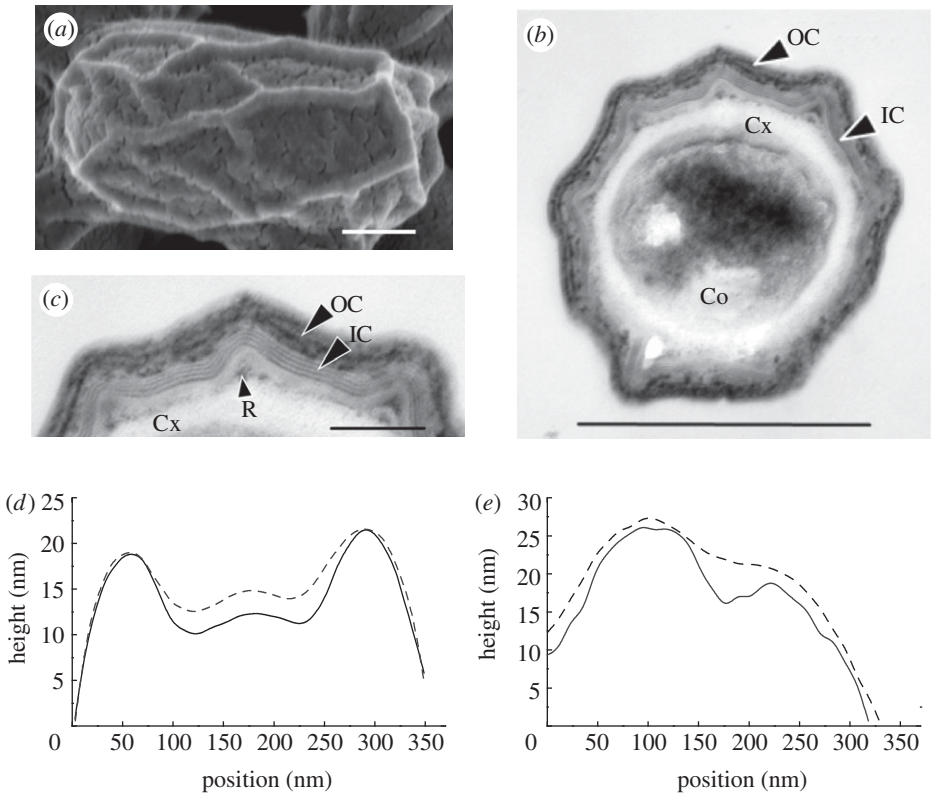

Figure 1. *B. subtilis* spore morphology. (*a*) Wild-type (strain PY79) spores were analysed by SEM, (*b,c*) TEM [2] (by fixation in glutaraldehyde and osmium, dehydration, embedment in Spurr's resin, and then thin-section transmission electron microscopy) and (*d*) with AFM height profiles. Separate height profiles obtained on *sterne* strain of *B. anthracis* are also given in (*e*). (*c*) Is a magnification part of (*b*). Cortex (Cx), inner coat (IC), outer coat (OC) and a ruck (R) are indicated in (*b*) and/or (*c*). The size bars indicate (*a*) 250, (*b*) 500 and (*c*) 100 nm. (The outer most layer of the coat, the crust [3] is not seen because of the fixation method). The spore has an ovoid shape with a long and a short axis [4]. (*d*) Height profiles measured along the short axis of a spore are recorded at low (35%, solid line) and high (95%, dashed line) relative humidity depict partial unfolding of the wrinkles at a high relative humidity. (*e*) Height profiles measured for *B. anthracis sterne* also exhibit partial unfolding of the wrinkles at a high relative humidity. To plot the two curves as closely as possible, an offset is added to the height profiles at a low relative humidity because the overall height of the spore increases with relative humidity. Note that the widths of the spores are larger than the widths of the curves in (*d,e*), which are plotted across the ridges on top of the spore.

the measured elastic modulus of the *B. subtilis* coat E approximately 13.6 GPa using an atomic force microscope [23] (AFM), and the energy of adhesion between the coat and the cortex, J, approximately 10 J m^{-2}, associated with non-specific electrostatic interactions between the cortex peptidoglycan [24] and the coat [24,25]. We note that the presence of outer forespore membrane can affect the strength of adhesion between the coat and cortex; however, we assumed that this membrane is no longer present in the mature spore.

The simulations show that as the rings shrink when the strain is larger than a critical threshold, c, the coat first buckles to form a symmetric wavy pattern around the cortex. This pattern then loses stability to delamination to form rucks (figure 2*a–c*). Once the rucks are formed, regaining spore volume does not result in reattachment of the coat. Rather, rucks unfold by decreasing their height and increasing their width (figure 2*d*), in qualitative agreement with our biological observations in figure 1*d*.

3. DISCUSSION

Wrinkles formed according to the mechanism in figure 2*a–c* are persistent. They do not readily attach back to the cortex, because they arise owing to a subcritical (nonlinear) instability. This has implications for the dormant spore, because it suggests that after completion of sporulation the spore volume can increase or decrease in response to ambient relative humidity without a significant resistance from the coat. The persistence of rucks ensures that the coat remains in a flexible state, despite large changes in the volume during dormancy [4,8,9], thereby providing a mechanism for maintaining structural integrity of the spore.

The origin of the coat's flexibility in the wrinkled state can be best understood by comparing the energy cost of bending and compression. If the coat were fully attached to the cortex, shrinkage of the spore interior owing to dehydration would have required the coat to be compressed. In contrast, our results indicate that the wrinkled coat expands and shrinks by changing its local curvature. While the energy cost of coat compression scales linearly with the coat thickness $U_{\text{compression}} \sim h$, the energy cost of bending scales with the third power of thickness $U_{\text{bending}} \sim h^3$. This means that as a layer of material gets thinner, bending becomes easier relative to compression. In the case of spores, reductions in the internal volume of the spore are best accommodated by folding and unfolding of wrinkles.

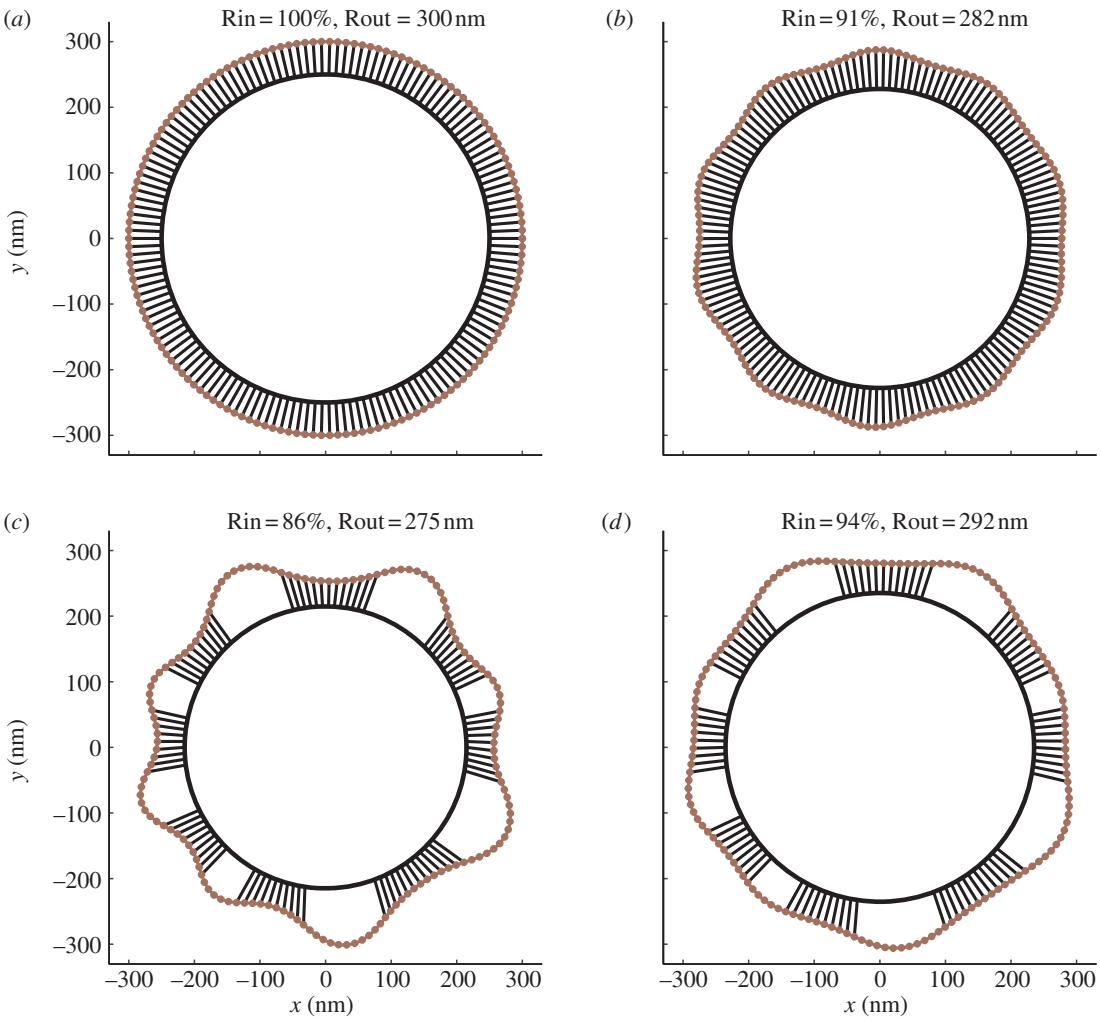

Figure 2. Model of formation of folds in the spore coat and their response to spore shrinking. (*a–c*) Simulation of the ruck formation as the radius of spore interior (Rin) shrinks during sporulation. Rin values are given as percentages of the initial value, 300 nm. Rout is the average outer diameter. Using bending and stretching modulus values estimated from thickness and mechanical measurements of the coat, the model predicts the emergence of rucks that are comparable in width, height and number to previous reports [26]. (*d*) Upon spore expansion, rucks formed during sporulation do not reattach readily, but rather decrease their height and increase their width. Details of simulation results are given in electronic supplementary material, movie S1. (Online version in colour.)

According to the wrinkle model, if the spore internal volume continues to increase, the wrinkles will eventually unfold completely. Beyond that point, the coat will begin to resist any further increase in volume. The biological observation in figure 1*d,e* that the rucks do not unfold completely suggests that this point is not reached even at very high relative humidity or at full hydration. Therefore, expansion of the dormant spore is not limited by the coat. Instead, the cortex of the dormant spore must have a limited ability to swell. Consistent with this view, *B. subtilis* spores lacking most of the coat owing to mutations in *cotE* and *gerE* [27] were not larger than wild-type spores at a high relative humidity (figure 3). This particular mutant no longer has the resistance properties of wild-type spores, especially to lysozyme; however, they maintain viability in laboratory environment [12,28]. The cortex's limited ability to swell can be explained by its rigidity, as our AFM-based mechanical measurements [23] on the *cotE gerE* mutant revealed an elastic modulus around approximately 6.9 GPa. A rigid cortex is also needed to sustain pulling forces on the coat, as well as in creating a tight girdle around the dehydrated core.

The observed architecture and dynamics of the coat and cortex of the dormant spore have important implications for the role of mechanical processes involved in germination, as well. In contrast to the dormant state, the wrinkles disappear in germinating spores [17,19]. Considering our model of wrinkle formation in the coat, a loss of cortex's ability to sustain the pulling forces exerted on the coat can lead to coat unfolding. Degradation of the cortex peptidoglycan during germination can plausibly facilitate this process. In fact, mutant spores that lack the capacity for the degradation of their cortex peptidoglycan still maintain wrinkles in their coats even after triggering germination and partial hydration of their core [29]. We note that according to this mechanism, the unfolding of the coat during germination is not necessarily driven by the expansion of the spore interior, but to a significant degree by the relaxation of the coat to its unfolded state. Because the unfolded and relaxed coat has a larger volume, relaxation of the coat could act like

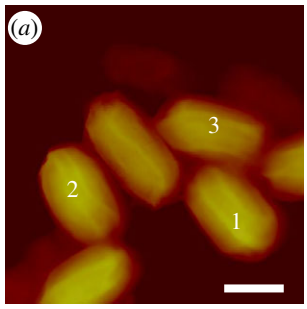

	low (nm)	high (nm)	difference (%)
1	725.2	749.7	3.4
2	720	759.1	5.4
3	649.3	670.1	3.2
average	698.2	726.3	4.0

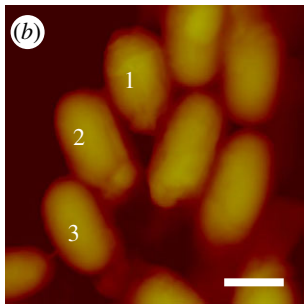

	low (nm)	high (nm)	difference (%)
1	707	733	3.7
2	683.5	709.6	3.8
3	667.8	693.9	3.9
average	686.1	712.2	3.8

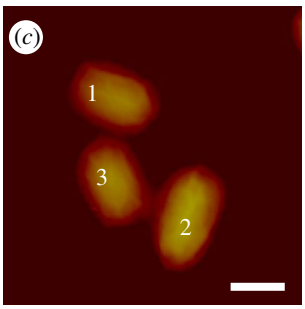

	low (nm)	high (nm)	difference (%)
1	786.9	821.4	4.4
2	843.5	915.1	8.5
3	820.3	846.4	3.2
average	816.9	861.0	5.4

Figure 3. (*a*) Height measurements on wild-type and (*b*) *cotE gerE* mutant of *B. subtilis*, and (*c*) *sterne* strain of *B. anthracis* at low (35%) and high humidity (95%). (*a–c*) Scale bars, 1 μm. Heights of spores marked on the AFM images are listed on the right for a low and a high relative humidity, together with the percentage of the differences and average values. The mutant *B. subtilis* spore lacks most of its coat; yet its expansion is comparable to wild-type spores. (Online version in colour.)

a pump, driving water into the spore. While hydration forces are likely to be primarily responsible for core hydration, a relaxed coat would allow core to absorb a larger volume of water.

Our findings raise the possibility that the mechanical properties of the coat participate in coat shedding, a prerequisite to outgrowth. The *B. subtilis* coat is shed as two hemispheres during or immediately following germination [19]. Possibly, the coat's mechanical properties play a role in holding these hemispheres together prior to germination, or facilitate their separation prior to the first cell division after germination.

4. CONCLUSION

Our findings suggest that the coat's global mechanical properties are critical not only during dormancy but also, strikingly, for rapidly breaking dormancy upon germination. We propose that the coat takes advantage of mechanical instabilities to fold into a wrinkled pattern during sporulation and accommodate changes in spore volume without compromising structural and biochemical integrity. Importantly, we argue that the emergent properties of the assembled coat, such as its elastic modulus and thickness [17], rather than specific individual molecular components, are responsible for coat flexibility. In this view, a functional coat can be built in a large number of ways and with diverse protein components. Such freedom in design parameters could facilitate evolutionary adaptation (particularly with respect to material properties) and the emergence of the wide range of molecular compositions and arrangements found among *Bacillus* spore coats [2,30]. The spore and its protective coat represent a simple paradigm likely used in diverse cell types [31] where regulated flexibility of a surface layer is adaptive, and may inspire novel applications for a controlled release of materials.

The authors acknowledge funding support from the Wyss Institute for Biologically Inspired Engineering, Rowland Junior Fellows Program, MacArthur Foundation and the Kavli Institute for Bionano Science and Technology.

REFERENCES

1 Nicholson, W. L., Munakata, N., Horneck, G., Melosh, H. J. & Setlow, P. 2000 Resistance of *Bacillus* endospores to extreme terrestrial and extraterrestrial environments.

Microbiol. Mol. Biol. Rev. **64**, 548–572. (doi:10.1128/MMBR.64.3.548-572.2000)
2 Traag, B. A. *et al.* 2010 Do mycobacteria produce endospores? *Proc. Natl Acad. Sci. USA* **107**, 878–881. (doi:10.1073/pnas.0911299107)
3 McKenney, P. T., Driks, A., Eskandarian, H. A., Grabowski, P., Guberman, J., Wang, K. H., Gitai, Z. & Eichenberger, P. 2010 A distance-weighted interaction map reveals a previously uncharacterized layer of the *Bacillus subtilis* spore coat. *Curr. Biol.* **20**, 934–938. (doi:10.1016/j.cub.2010.03.060)
4 Plomp, M., Leighton, T. J., Wheeler, K. E. & Malkin, A. J. 2005 The high-resolution architecture and structural dynamics of *Bacillus* spores. *Biophys. J.* **88**, 603–608. (doi:10.1529/biophysj.104.049312)
5 Driks, A. 1999 The *Bacillus subtilis* spore coat. *Microbiol. Mol. Biol. Rev.* **63**, 1–20.
6 Driks, A. 2009 The *Bacillus anthracis* spore. *Mol. Aspects Med.* **30**, 368–373. (doi:10.1016/j.mam.2009.08.001)
7 Henriques, A. O. & Moran, C. P. 2007 Structure, assembly and function of the spore surface layers. *Ann. Rev. Microbiol.* **61**, 555–588. (doi:10.1146/annurev.micro.61.080706.093224)
8 Driks, A. 2003 The dynamic spore. *Proc. Natl Acad. Sci. USA* **100**, 3007–3009. (doi:10.1073/pnas.0730807100)
9 Westphal, A. J., Price, P. B., Leighton, T. J. & Wheeler, K. E. 2003 Kinetics of size changes of individual *Bacillus thuringiensis* spores in response to changes in relative humidity. *Proc. Natl Acad. Sci. USA* **100**, 3461–3466. (doi:10.1073/pnas.232710999)
10 Setlow, P. 2003 Spore germination. *Curr. Opin. Microbiol.* **6**, 550–556. (doi:10.1016/j.mib.2003.10.001)
11 Beall, B., Driks, A., Losick, R. & Moran Jr, C. 1993 Cloning and characterization of a gene required for assembly of the *Bacillus subtilis* spore coat. *J. Bacteriol.* **175**, 1705–1716.
12 Driks, A., Roels, S., Beall, B., Moran, C. P. J. & Losick, R. 1994 Subcellular localization of proteins involved in the assembly of the spore coat of *Bacillus subtilis*. *Genes Dev.* **8**, 234–244. (doi:10.1101/gad.8.2.234)
13 Levin, P. A., Fan, N., Ricca, E., Driks, A., Losick, R. & Cutting, S. 1993 An unusually small gene required for sporulation by *Bacillus subtilis*. *Mol. Microbiol.* **9**, 761–771. (doi:10.1111/j.1365-2958.1993.tb01736.x)
14 Roels, S., Driks, A. & Losick, R. 1992 Characterization of spoIVA, a sporulation gene involved in coat morphogenesis in *Bacillus subtilis*. *J. Bacteriol.* **174**, 575–585.
15 Bradley, D. E. & Franklin, J. G. 1958 Electron microscope survey of the surface configuration of spores of the genus *Bacillus*. *J. Bacteriol.* **76**, 618–630.
16 Bradley, D. E. & Williams, D. J. 1957 An electron microscope study of the spores of some species of the genus *Bacillus* using carbon replicas. *J. Gen. Microbiol.* **17**, 75–79. (doi:10.1099/00221287-17-1-75)
17 Chada, V. G., Sanstad, E. A., Wang, R. & Driks, A. 2003 Morphogenesis of *Bacillus* spore surfaces. *J. Bacteriol.* **185**, 6255–6261. (doi:10.1128/JB.185.21.6255-6261.2003)
18 Cerda, E. & Mahadevan, L. 2003 Geometry and physics of wrinkling. *Phys. Rev. Lett.* **90**, 074302. (doi:10.1103/PhysRevLett.90.074302)
19 Santo, L. Y. & Doi, R. H. 1974 Ultrastructural analysis during germination and outgrowth of *Bacillus subtilis* spores. *J. Bacteriol.* **120**, 475–481.
20 Kolinski, J. M., Aussillous, P. & Mahadevan, L. 2009 Shape and motion of a ruck in a rug. *Phys. Rev. Lett.* **103**, 174302. (doi:10.1103/PhysRevLett.103.174302)
21 Wang, R., Krishnamurthy, S. N., Jeong, J. S., Driks, A., Mehta, M. & Gingras, B. A. 2007 Fingerprinting species and strains of *Bacilli* spores by distinctive coat surface morphology. *Langmuir* **23**, 10 230–10 234. (doi:10.1021/la701788d)
22 Silvaggi, J. M., Popham, D. L., Driks, A., Eichenberger, P. & Losick, R. 2004 Unmasking novel sporulation genes in *Bacillus subtilis*. *J. Bacteriol.* **186**, 8089–8095. (doi:10.1128/JB.186.23.8089-8095.2004)
23 Sahin, O. & Erina, N. 2008 High-resolution and large dynamic range nanomechanical mapping in tapping-mode atomic force microscopy. *Nanotechnology* **19**, 445717. (doi:10.1088/0957-4484/19/44/445717)
24 Mera, M. U. & Beveridge, T. J. 1993 Mechanism of silicate binding to the bacterial cell wall in *Bacillus subtilis*. *J. Bacteriol.* **175**, 1936–1945.
25 Chen, G., Driks, A., Tawfiq, K., Mallozzi, M. & Patil, S. 2010 *Bacillus anthracis* and *Bacillus subtilis* spore surface properties as analyzed by transport analysis. *Colloids Surf. B Biointerfaces* **76**, 512–518. (doi:10.1016/j.colsurfb.2009.12.012)
26 McPherson, D., Kim, H., Hahn, M., Wang, R., Grabowski, P., Eichenberger, P. & Driks, A. 2005 Characterization of the *Bacillus subtilis* spore coat morphogenetic protein CotO. *J. Bacteriol.* **187**, 8278–8290. (doi:10.1128/JB.187.24.8278-8290.2005)
27 Ghosh, S., Setlow, B., Wahome, P. G., Cowan, A. E., Plomp, M., Malkin, A. J. & Setlow, P. 2008 Characterization of spores of *Bacillus subtilis* that lack most coat layers. *J. Bacteriol.* **190**, 6741–6748. (doi:10.1128/JB.00896-08)
28 Setlow, P. 2006 Spores of *Bacillus subtilis*: their resistance to and killing by radiation, heat and chemicals. *J. Appl. Microbiol.* **101**, 514–525. (doi:10.1111/j.1365-2672.2005.02736.x)
29 Popham, D. L., Helin, J., Costello, C. E. & Setlow, P. 1996 Muramic lactam in peptidoglycan of *Bacillus subtilis* spores is required for spore outgrowth but not for spore dehydration or heat resistance. *Proc. Natl Acad. Sci. USA* **93**, 15 405–15 410. (doi:10.1073/pnas.93.26.15405)
30 Aronson, A. I. & Fitz-James, P. 1976 Structure and morphogenesis of the bacterial spore coat. *Bacteriol. Rev.* **40**, 360–402.
31 Elbaum, R., Gorb, S. & Fratzl, P. 2008 Structures in the cell wall that enable hygroscopic movement of wheat awns. *J. Struct. Biol.* **164**, 101–107. (doi:10.1016/j.jsb.2008.06.008)

Electronic Supplementary Materials

Supplementary Section 1: Modeling and Simulations

Methodology: In order to simulate ruck formation when the spore shrinks, we model the spore as two concentric rings (or polygons) of radii R_1 and R_2 that are comprised of N edges and N vertices. The outer polygon models the coat while the inner polygon models the core and cortex. For each vertex on the inner polygon there is a corresponding vertex on the outer polygon, lying on the same radial line. The polygon asymptotes a circle as N increases. In the simulation, the inner polygon oscillates sinusoidally between the initial radius R_1 and minimum radius R_2. We did not allow bending and stretching. Thus, each cortex vertex oscillates between R_1 and R_2 with a characteristic period T_c. The outer polygon, modeling the coat, has more complex mechanical behavior. In addition to the bending and stretching energy associated with the elastic extensible ring [1], we added substrate energy between the two concentric rings to model the adhesion force between the coat and cortex, which is Hookean and of finite range. Finally, we added a shearing penalty between the two layers to prevent the two polygons from sliding relative to one another.

Numerical Model

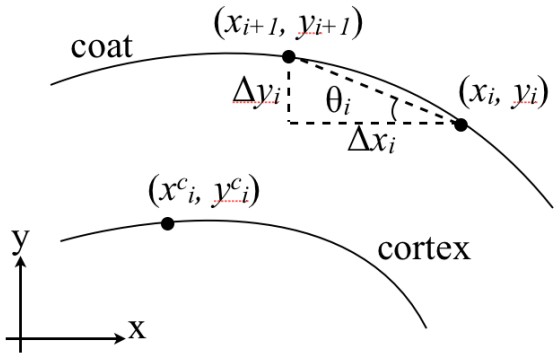

Figure S1: Model and notations

The cross section of the initial spore is modeled by two concentric circular rings, with inner radius R_1 and outer radius R_2. We will label the outer vertices by $(x_i; y_i)$ and the inner vertices by $(x_i^c; y_i^c)$ (figure S1). Let us define $\Delta x_i = x_{i+1} - x_i$, $\Delta y_i = y_{i+1} - y_i$.Then, the length of an outer edge is given by $\Delta r_i = \sqrt{(\Delta x_i^2 + \Delta y_i^2)}$. The angle between the i^{th} edge (tangent vector of i^{th} vertex) and the x-axis is given by θ_i, where $\tan\theta_i = \Delta y_i/\Delta x_i$. Similar notations hold for the inner polygon, with the addition of a superscript c. The total energy of the coat (outer layer) is given by U(coat):

$$U(coat) = U_{bend} + U_{stretch} + U_{substrate} + U_{shear}, \quad (1)$$

Where

$$U_{bend} = -\kappa_b \sum_i \cos(\theta_{i+1} - \theta_i - \delta) \quad , \delta = \frac{2\pi}{N}, \tag{2}$$

$$U_{stretch} = \frac{1}{2}\kappa_h \sum_i \left(\frac{\Delta r_i - \ell}{\ell}\right)^2 \quad , \ell = 2R_2 \sin\frac{\pi}{N}, \tag{3}$$

$$U_{substrate} = \frac{1}{2}\kappa_h \sum_i (r_i - r_i^c)^2 \quad , r_i = \sqrt{x_i^2 + y_i^2}, \tag{4}$$

$$U_{shear} = -\kappa_h \sum_i \cos(\theta_i^c - (i-1)\delta). \tag{5}$$

U_{bend} and $U_{stretch}$ denote the bending and stretching energy respectively, while $U_{substrate}$ denotes the adhesive restoring energy between the cortex and the coat. r_i^c is the equilibrium separation and U_{shear} is the shear energy when the two layers slide relative to one another.

The outer (coat) vertices (x_i; y_i) evolve via over-damped dynamics

$$\eta \frac{dx_i}{dt} = -\frac{\partial U(\text{coat})}{\partial x_i}, \quad \eta \frac{dy_i}{dt} = -\frac{\partial U(\text{coat})}{\partial y_i}, \tag{6}$$

On the other hand, since the inner polygon undergoes a simple harmonic motion $R_{core}(t) = R_m + A\cos\omega t$, where $R_m=(R_1+R_2)/2$ and $A = (R_2 - R_1)/2$, the inner vertices (x_i^c; y_i^c) move via

$$\frac{dx_i^c}{dt} = -\omega A \sin(\omega t)\cos(\phi_i^c), \tag{7}$$

$$\frac{dy_i^c}{dt} = -\omega A \sin(\omega t)\sin(\phi_i^c), \tag{8}$$

Where ϕ_i^c is the angle of the i^{th} inner vertice relative to the x-axis. Additionally, the Hookean adhesion force is assumed to be of finite range (Fig. S2) and the bonds linking two rings will break if the force exceeds some cutoff separation x^*, where $x^* = \max(r_i - r_i^c)$ denotes the maximum extension of the spring at each vertex before it breaks. We can relate the elastic modulus for the substrate κ_s (mentioned in the previous section) to the adhesion constant J. If we assume that there is one spring per edge, then

$$\frac{1}{2}\kappa_s (x^*)^2 = \frac{1}{2}\kappa_s [max(r_i - r_i^c)]^2 = J\ell \tag{9}$$

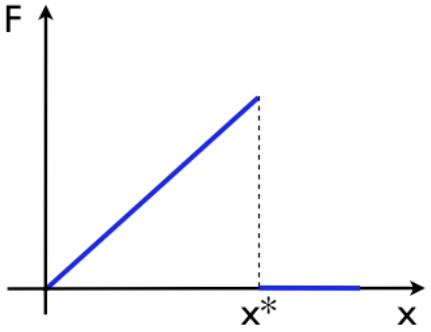

Figure S2: Finite range Hookean restoring force between the coat and substrate (cortex)

Once the simulation starts running, the inner core region will shrink to its minimum radius R_1, resulting in the outer coat being pulled inwards due to the Hookean adhesion force between the two layers and forming complex patterns of wrinkles/rucks.

Parameters for numerical simulations

Next, we would like to relate the numerical values to experimentally observable quantities. Since $\kappa_h' = Eh$ and $\kappa_b' \sim Eh^3$ where E = 13.9 GPa is the elastic constant and $h \sim 40\ \mathrm{nm}$ is the thickness of the coat, we find that $\kappa_s' \sim 500\ \mathrm{N/m}$ and $\kappa_b' \sim 9 \cdot 10^{-13}\ \mathrm{Nm}$. $J' \sim 1\mathrm{N/m}$. Here the prime on the parameters represent physical values from the corresponding numerical values used in the simulation. By matching the analytical expressions for bending and stretching energy to the numerical expressions given by eqs. (3) and (4), we find

$$\kappa_s \propto \frac{\kappa_s'}{\ell}, \qquad \kappa_b \propto \frac{\kappa_b'}{\ell} \tag{10}$$

The numerical parameters are listed in the Table S1.

Name	Description	Numerical values used in simulation
N	Number of discretization	150
κ_b	Bending modulus	2×10^6
κ_h	Stretching modulus	10^5
κ_s	Adhesion modulus	360
κ_r	Shearing Modulus	10^6
T_c	Period of cortex oscillation	2
δ	Equilibrium angle	2π/N
η	Damping constant	1
R_1	Initial size of inner coat	250
R_2	Initial size of outer coat	300
A	Amplitude of cortex oscillation	18
J	Adhesion constant	52000
	Equilibrium length of outer edge	$2R_2 \sin(\pi/N)$
x^*	Maximum extension of bonds	$\sqrt{2J\ell/\kappa_s}$

Table S1: Descriptions and values of the parameters used in simulations.

Size of a ruck

The critical size of a ruck can be estimated in two ways. Firstly, let us consider the size of a ruck in soft, extensible film that adheres to a substrate [1,2]. The energy per unit width of a film of length l is $W = U_a + U_b + U_c$ where $U_a \sim Jl$ is the adhesive energy, $U_b \sim (Eh^3)\Delta^2/l^3 \sim (Eh^3)\varepsilon/l^2$ is the bending energy and $U_c \sim (Eh)\varepsilon^2/l$ is the compressive strain energy (h is the thickness of the film). The longitudinal displacement ε is related to the lateral displacement Δ via $\Delta \sim (\varepsilon l)^{1/2}$. Minimizing $W(\varepsilon, l)$ with respect to ε and l yields scaling laws for the critical compression $\varepsilon_c \sim (Jh^3/E)^{1/4}$ required to form a ruck of critical size $l_c \sim (Eh^5/J)^{1/4}$. We measured the elastic modulus E of the coat to be ~13.9 GPa using AFM. Using the typical dimensions of a spore ruck $l_c \sim$ 100nm, $\Delta \sim$ h ~ 30nm, we estimate that $\varepsilon \sim$ 9 nm and J ~ 4 N/m, which are reasonable figures.

Alternatively, if we assume that the film is inextensible and is compressed an amount ε by an applied stress F in the longitudinal direction, then the energy per unit width of the film of length l is $W = U_a + U_b + U_c$ where $U_a \sim Jl$ is the adhesive energy, $U_b \sim (Eh^3)\varepsilon/l^2$ is the bending energy and $U_c \sim F\varepsilon$ is the energy due to the applied force. Minimizing $W(l)$ with respect to l yields the scaling law for the critical ruck size $l_c \sim (Eh^3\varepsilon/J)^{1/3}$. Assuming ε to be a few nanometers, then J is approximately 1.8 N/m.

Supplementary Section 2: Movie 1

Simulation of the ruck formation as the radius of spore interior shrinks during sporulation. Coat is represented with the dark red curve and spore interior is represented with the black circle. Radial lines between the coat and spore interior represent the adhesion between the coat and cortex. The simulated geometry of the spore cross section is plotted as the radius of spore interior (Rin) gradually decreases and then increases. Rout is the average coat diameter. The graph on the left side shows the variation of Rout in response to Rin. The dark red circle marks the values of Rin and Rout that correspond to the geometry displayed on the right. Note that upon spore expansion, rucks formed during initial shrinkage (corresponding to sporulation) do not reattach readily, but rather decrease their height and increase their width.

Supplementary Section 3: Surface topography and height measurements of bacterial spores

We have used an atomic force microscope to observe changes in surface topography of wild type and mutant spores at low and high relative humidity. Samples are prepared by pipetting a droplet of spore suspension (~5 μL) onto a freshly cleaved mica substrate followed by air drying. A Multimode AFM system (Bruker AXS, Santa Barbara, CA) equipped with an environmental chamber to control relative humidity is used. Measurement of elastic modulus of the spore coat is also carried out in this system using a previously reported method [3].

In addition to the height profiles and topography images given in Figure 1(d,e) and Figure 3, figure S3 shows height profiles across a *cotE gerE* mutant of *B. subtilis* at low and high relative humidity.

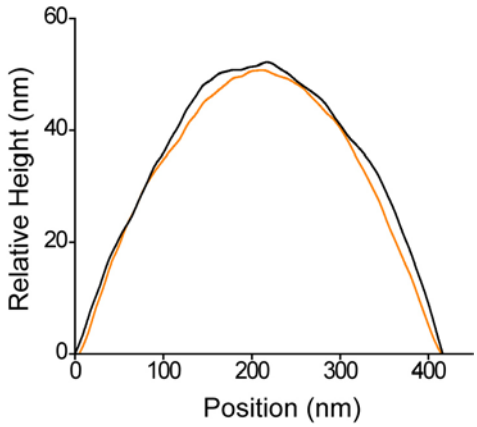

Figure S3. Height profiles at low (35%, black) and high (95%, orange) relative humidity on *cotE gerE* mutant of B. *subtilis* (b). Horizontal and vertical axes are arbitrarily referenced. The average heights of the spores increase at high humidity. To compare local curvatures, the profile obtained at high relative humidity is vertically offset. The profiles show that the surface of the *cotE gerE* mutant of *B. subtilis* remains smooth at both high and low levels of relative humidity.

Supplementary Section 4: Identification of coat proteins not required for significant coat stiffness

We do not know which coat protein(s) are required for the high elastic modulus of the coat. To at least partially clarify this question, we took advantage of previous results showing that the *B. subtilis cotE* mutant spore coat is unfolded, lacks most if not all outer coat proteins and has an only partially intact inner coat[4-8]. The unfolded state of the *cotE* mutant coat could be due to a significant decrease in coat stiffness or its adhesion to the cortex. Therefore, analysis of the *cotE* mutant spore coat elastic modulus might allow us to address the roles of a subset of coat proteins in spore mechanical properties. We found the elastic modulus of the *cotE* mutant coat to be ~6 GPa, which is comparable to that of the wild type coat and inconsistent with a significant reduction in stiffness due to the mutation. Therefore, most or all the outer coat proteins are dispensable for a significantly stiff coat. Additionally, we infer that in *cotE* mutant spores, defects in the inner coat prevent it from folding and/or properly adhering to the cortex.

Supplementary Section 5: Localization of SpoIVA to the underside of the coat.

The variation in coat folding patterns from spore to spore suggests that coat-cortex interactions are non-specific. Possibly, these are nonspecific electrostatic interactions between the cortex [8] and coat [9]. The coat protein SpoIVA could plausibly make a significant fraction of these interactions, as it is argued to connect the coat to the outer forespore membrane [10-14]. To address whether SpoIVA is exposed on the coat-interior surface, we used immunofluorescence microscopy [14] with anti-SpoIVA antibodies [17] to analyze fluorescently labeled coats shed during germination (figure S4). These data argue that SpoIVA is exposed on the interior (concave) face of shed coat material, consistent with the possibility that SpoIVA contributes to coat-cortex interactions.

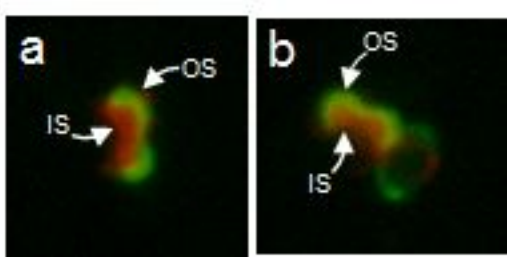

Figure S4. Immunofluorescence localization of SpoIVA to the inner surface of shed coats (a,b). Spores bearing CotB-GFP (*cotB-gfpωcotB*) were incubated in LB medium for 90 minutes to promote outgrowth, the shed coats were reacted with anti-SpoIVA antibody followed by a FITC-conjugated secondary antibody and then imaged by epifluorescence microscopy [15]. GFP fluorescence is colored green and fluorescence due to anti-SpoIVA binding is colored red. The shed coat appears as two partially separated hemispheres, like a cracked-open egg shell. Prior to shedding, when the coat is a contiguous shell, the inner surface (IS) of each hemisphere contacts the spore's interior structures. CotB is known to be on the spore outer surface (OS) [16]

Additional References:

1. Landau LD & Lifshitz EM (1986) Theory of Elasticity (Pergamon, New York) 3 Ed.
2. Kolinski JM, Aussillous P, Mahadevan L. Shape and motion of a ruck in a rug. Phys Rev Lett. 2009 Oct 23;103(17):174302.
3. Sahin O & Erina N (2008) High-resolution and large dynamic range nanomechanical mapping in tapping-mode atomic force microscopy. Nanotechnology 19(44):447717.
4. Zheng L, Donovan WP, Fitz-James PC, & Losick R (1988) Gene encoding a morphogenic protein required in the assembly of the outer coat of the *Bacillus subtilis* endospore. Genes Dev. 2:1047-1054.
5. Little S & Driks A (2001) Functional analysis of the *Bacillus subtilis* morphogenetic spore coat protein CotE. Mol. Microbiol. 42:1107-1120.
6. Bauer T, Little S, Stöver AG, & Driks A (1999) Functional regions of the *Bacillus subtilis* spore coat morphogenetic protein CotE. J. Bacteriol. 181:7043-7051.
7. Kim H, et al. (2006) The *Bacillus subtilis* spore coat protein interaction network. Mol. Microbiol. 59:487-502.
8. Mera MU & Beveridge TJ (1993) Mechanism of silicate binding to the bacterial cell wall in *Bacillus subtilis*. J. Bacteriol. 175:1936-1945.
9. Chen G, Driks A, Tawfiq K, Mallozzi M, & Patil S (2010) *Bacillus anthracis* and *Bacillus subtilis* Spore Surface Properties as analyzed by transport analysis. Colloids and Surfaces B: Biointerfaces 76:512-518.
10. Roels S, Driks A, & Losick R (1992) Characterization of spoIVA, a sporulation gene involved in coat morphogenesis in *Bacillus subtilis*. J. Bacteriol. 174:575-585.

11. Piggot PJ & Coote JG (1976) Genetic aspects of bacterial endospore formation. Bacteriol. Rev. 40:908-962.

12. Driks A, Roels S, Beall B, Moran CPJ, & Losick R (1994) Subcellular localization of proteins involved in the assembly of the spore coat of *Bacillus subtilis*. Genes Dev. 8:234-244.

13. Price KD & Losick R (1999) A four-dimensional view of assembly of a morphogenetic protein during sporulation in *Bacillus subtilis*. J. Bacteriol. 181:781-790.

14. Pogliano K, Harry E, & Losick R (1995) Visualization of the subcellular location of sporulation proteins in *Bacillus subtilis* using immunofluorescence microscopy. Mol. Microbiol. 18:459-470.

15. McPherson D, et al. (2005) Characterization of the *Bacillus subtilis* spore coat morphogenetic protein CotO. J. Bacteriol. 187:8278-8290.

16. Isticato R, Cangiano G, Tran HT, Ciabattini A, Medaglini D, Oggioni MR, De Felice M, Pozzi G, Ricca E. (2001)Surface display of recombinant proteins on *Bacillus subtilis* spores. J. Bacteriol. 183:6294-6301.

17. Catalano FA, Meador-Parton J, Popham DL, & Driks A (2001) Amino acids in the *Bacillus subtilis* morphogenetic protein SpoIVA with roles in spore coat and cortex formation. J. Bacteriol. 183:1645-1654.